A novel approach to developer-soluble anti-reflective coatings for 248-nm lithography

Ramil-Marcelo L. Mercado, Joyce A. Lowes, Carlton A. Washburn, Douglas J. Guerrero
Brewer Science, Inc., 2401 Brewer Dr., Rolla, MO, USA 65401

ABSTRACT

A novel approach to developer-soluble bottom anti-reflective coatings (BARCs) for 248-nm lithography was demonstrated. The BARC formulations are photosensitive, dye-filled systems incorporated with a polymer binder. The films are generated by thermally crosslinking the polymer matrix, and are then photochemically decrosslinked in order to render them soluble in developer solutions. The BARCs are compatible with solvents commonly used in the industry. Easy modification of the films with regard to optical properties for potential use with various substrates was also demonstrated. The BARCs exhibit anisotropic development in aqueous tetramethylammonium hydroxide (TMAH) solutions subsequent to simulated photoresist application, exposure, and post-exposure bake.

Keywords: 248 nm, developer soluble, photosensitive, anti-reflective coatings

1. INTRODUCTION

With the IC industry moving to and implementing the 65 nm and 45 nm device nodes, the accompanying critical dimension (CD) control required for implant layers has increased. At the 65 nm node, implant CD is expected to be at 180 nm or less,[1,2] and is about 150 nm for the 45 nm node.[2] KrF lithographic processes are currently used for implant layers, with the foremost approach using dyed resist along with a top anti-reflective coating (TARC).[1] This approach, however, will no longer provide adequate performance beyond the 65 nm node.[2] In addition, ion implantation is usually done on substrates that have topography, and the topography causes large CD variations for a resist (dyed or undyed) with a TARC.[2,9]

Bottom anti-reflective coatings (BARCs) have traditionally offered better CD control than the dyed resist-TARC combination.[1-6,9,10] It has also been shown that a BARC will sufficiently cover substrates with 150 nm step heights and still provide adequate reflection control, leading to better CD control.[9] The drawback with this process is that organic BARCs are usually removed in a reactive ion etching (RIE) step, which adds cost and may damage the implanted substrate. As a result, developer-soluble BARCs have been developed such that the BARC layer is removed in the same step as the photoresist removal, which eliminates the need for an RIE step.[1-8]

Previous generations of developer-soluble BARCs are based on polyamic acids.[3-5] These systems have development rates that are determined by the BARC post-application bake (BARC PAB) temperature, and their development behavior in tetramethylammonium hydroxide (TMAH) developer is isotropic. Therefore, the lithographic profiles are largely determined by both temperature and development time, limiting the acceptable processing window. Quasi-anisotropic development behavior has been demonstrated in polyamic acid BARCs by utilizing a bilayer system that exhibits different development rates.[3] This method, however, adds another sequence of BARC coating and PAB steps to the process, and is still limited by the acceptable BARC bake window.

Anisotropically developing BARCs have been reported previously, both for use in KrF[1,2,7] and ArF[2,6,8,9] lithography. Anisotropic development has been achieved by making the BARCs photosensitive to the wavelength of interest.

One approach[1,2] that has been employed is to make the equivalent of a very heavily dyed, thin photoresist. Such a BARC is comprised of a polymer with highly absorbing groups and acid labile functionalities, and incorporates photoacid generators (PAGs) and amine quenchers in its formulations. This approach has shown good lithographic performance and wide process windows[1,2], but the BARC formulations themselves are limited in that they are necessarily made to avoid solubility in common photoresist solvents such as propylene glycol monomethyl ether (PGME) and propylene glycol methyl ether acetate (PGMEA). While this formulation design minimizes intermixing with the photoresist, such BARCs present potential processing and logistical problems in the fab. PGMEA is also used as an edge bead remover (EBR), and these BARCs would need separate spin bowls and drain lines to prevent precipitation of the polymers.

Another approach has been to incorporate photocleavable functional groups into polymer backbones, such as polycarbonates and polysulfones.[7] These polymers are initially soluble in ethyl lactate (EL) and PGMEA, but are rendered insoluble by baking above 170°C. Micron-scale patterning ability was demonstrated in these systems.

A third approach to achieve anisotropically developing BARCs was demonstrated in 2006,[6,8] although this approach was geared for ArF lithography. In this method, a polymer with carboxylic acid moieties was combined with a multifunctional crosslinker, PAG, quencher, and solvent in a formulation. The components are soluble in common industry solvents prior to the BARC PAB. The baking step produces a crosslinked film, which minimizes interactions with the photoresist. The BARC is then processed in the same steps as the photoresist (i.e., exposure, post-exposure bake, develop) to produce the lithographic image. This crosslinking approach thus maintains compatibility with the EBR solvents and processes.

In this work, the authors describe yet another approach, focused primarily on 248-nm lithographic needs, of developing BARCs that are photosensitive in nature and thus are expected to have anisotropic development behavior.

2. EXPERIMENTAL

2.1 Chemistry

The formulations consist of polymers with carboxylic acid groups, oligomeric dyes, crosslinker, PAG, quencher, and industry-accepted solvents. The polymers themselves are essentially transparent to 248-nm radiation. The BARC films are initially soluble and are rendered insoluble by the BARC PAB. This process is depicted graphically in Figure 1.

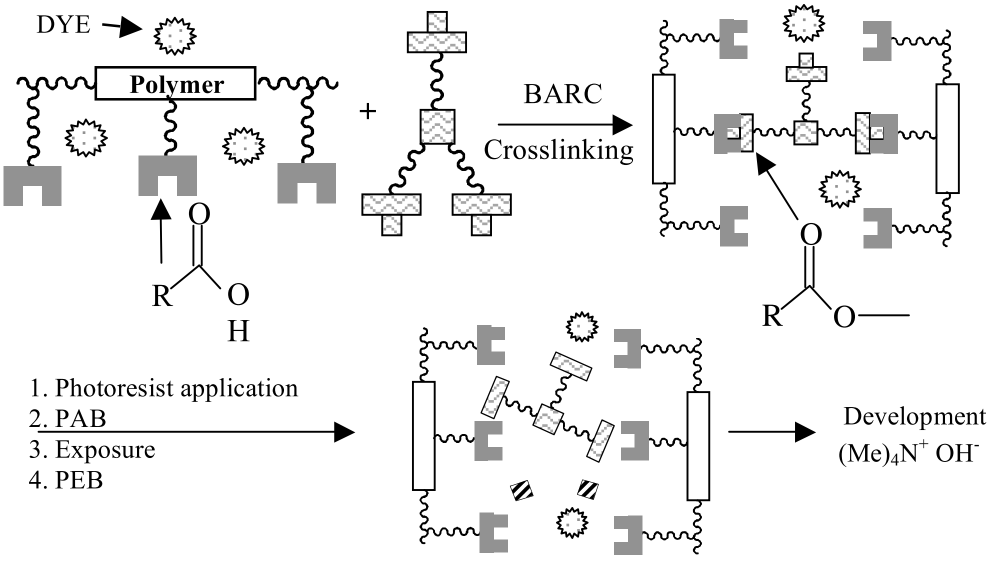

Figure 1. Graphical depiction of the BARC crosslinking and photo-induced decrosslinking process.

Polymer molecular weights were obtained using a Waters gel Permeation chromatograph, with a Polymer Laboratories PLgel 5-μm mixed bed column. Tetrahydrofuran was used as the mobile phase, and polystyrene was used as the standard.

2.2 PROLITH Modeling

PROLITH version 9.3.3.14 from KLA-Tencor was used for all modeling work.

2.3 Experimental Design

Design-Expert® version 6.0.5 was used for developing the experimental designs described. A simplex lattice mixture design with 3 factors and 6 levels was used for both formulation experiments.

The amounts of polymer, dye, and crosslinker were varied in the first set of experiments. The samples were evaluated for refractive index (*n*), imaginary component of the refractive index (*k*), EL stripping, and developer stripping. The optimum formulation was then used for the second set of experiments.

The amounts of PAG 1, PAG 2, and quencher were varied in the second set of experiments. The rest of the formulation components (polymer, crosslinker, and solvent) were held constant.

2.4 Contrast curve generation and topography clear-out

Film thickness on a 4-inch silicon substrate was measured with a LSE-WS Stokes WAFERSCAN™ ellipsometer (Gaertner Scientific Corporation). BARC films were baked at 160°C for 60 seconds and subjected to a simulated resist PAB (110°C for 60 seconds). The BARC film was exposed on an Oriel DUV broadband light source with a 248 nm bandpass filter. The exposure technique is shown in a diagram (Figure 2). A PEB of 110°C for 60 seconds was applied, and then the BARC was developed for 60 seconds using PD523AD.

A similar technique was used to evaluate how the BARC film would be removed from topography. Topography chips had 80-nm-wide spaces and 100-nm depths.

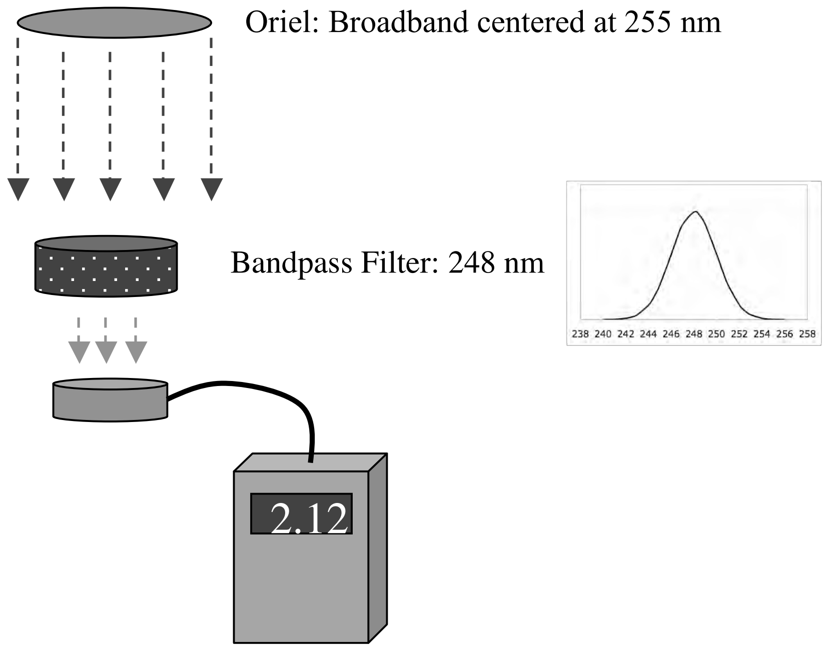

Figure 2. Experimental setup for BARC photochemical evaluation with a broadband light source.

2.5 Processing and Lithography

Ethyl lactate was used as a stripper solvent to determine the minimum temperature required for baking the BARC while maintaining solvent resistance after coating and curing. The solvent was allowed to puddle on the film for 20 seconds, and was spin dried. The film thickness was compared before and after contact with solvent. BARC bakes were 160°C for 60 seconds. Optical constants *n* and *k* were measured at 248 nm using a J. A. Woollam Co. VUV-VASE® variable-angle spectroscopic ellipsometer.

The BARC formulations were coated and baked on silicon substrates. The BARC thickness used was 80 nm, which is the thickness at the first reflectivity maximum. M91Y was the photoresist used. Target CD was 180 nm (1:1 L/S), resist thickness was 410 nm, resist PAB was at 130°C for 60 seconds, resist PEB was at 130°C for 60 seconds, annular illumination (NA: 0.7, σ: 0.875/0.575), and developer used was OPD 262 (40 seconds).

3. RESULTS AND DISCUSSION

3.1 Formulation Design

The purpose of the first set of experiments was to determine if an acceptable BARC formulation could be obtained by varying three components of the formulation: polymer, dye, and crosslinker. The BARC film should have an acceptable absorbance, as represented by the *k* value, and the film must also be essentially insoluble in the photoresist solvent (simulated by the EL strip test) after baking. In addition, the film must also be insoluble in developer solution. Table 1 shows the actual amounts of each component used in this set of experiments.

Table 1. Formulation compositions used to optimize BARC stripping and optical parameters.

Component 1	Component 2	Component 3
A: Polymer	B: Dye	C: Crosslinker
g	g	g
0.1006	0.6033	0.4737
0.3016	0.3016	0.2368
0.2011	0.3016	0.4737
0.1006	0.9050	0.2368
0.1347	0.7059	0.3174
0.2353	0.4042	0.3174
0.1006	0.3016	0.7106
0.3016	0.3016	0.2368
0.2011	0.6033	0.2368
0.1006	0.3016	0.7106
0.1669	0.5007	0.3932
0.1006	0.9050	0.2368
0.1669	0.5007	0.3932
0.1347	0.4042	0.5542

Results of the combined developer, EL strip and optical parameter tests are shown in Figure 3.

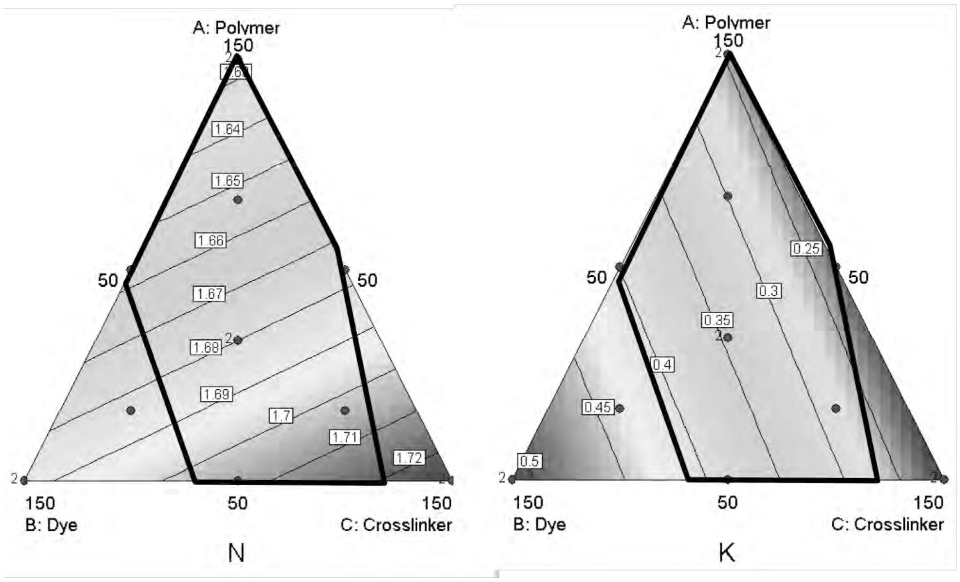

Figure 3. Triangle diagrams showing components and relative amounts (%). The area delineated by the black borders indicates acceptable formulation ranges.

As shown in Figure 3, a relatively broad area was obtained from which acceptable BARC formulations could be made. Refractive index, *n*, values range from 1.62-1.71, while *k* values range from 0.23 to 0.42. The area bordered in black indicates the formulation compositions that exhibit minimal stripping in EL and TMAH-based developer.

Arbitrarily setting a desired *k* value of 0.4 and ignoring *n*, the optimum formulation obtained is then one comprised (in %) relative to each component: polymer: 50, dye: 105, and crosslinker: 95. This formulation was then used in the second set of experiments wherein the polymer, dye, crosslinker, and solvent amounts were held constant and the amount of 2 PAGs and the quencher were varied. These amounts are shown in Table 2.

Table 2. Formulation compositions used to determine BARC lithographic performance.

Component 1	Component 2	Component 3
A: Quencher	B: PAG 1	C: PAG 2
g	g	g
0.0116	0	0.0959
0.0274	0.0767	0.0163
0.1043	0	0
0.0274	0.0195	0.0643
0.0580	0.0572	0
0.0116	0.1140	0
0.0116	0	0.0959
0.1043	0	0
0.0116	0.1145	0
0.0737	0.0195	0.0163
0.0580	0	0.0480
0.0422	0.0378	0.0317
0.0580	0.0572	0
0.0116	0.0572	0.0480

The formulation used did not show appreciable stripping in EL prior to the addition of PAG and quencher. However, this was no longer the case after both components were added to the formulations. These results are shown in Figure 4. The area in the lower left corner represents formulations that can be obtained without causing BARC film loss in EL (≤5 nm of film loss). This experiment shows that the addition of ionic components and basic quencher interferes with the crosslinker mechanism (ester formation).

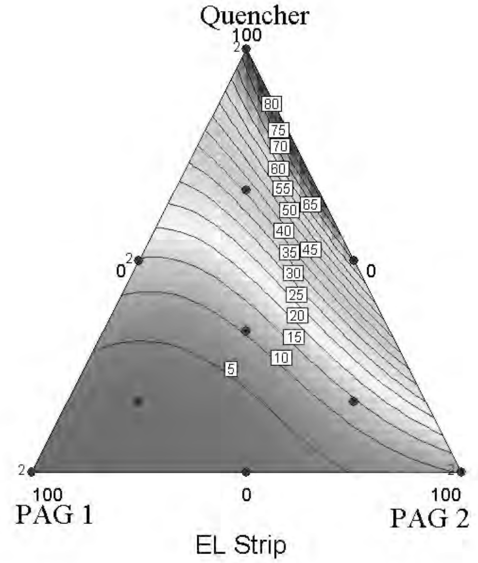

Figure 4. EL strip test results for BARC formulations. Triangle corners represent maximum amounts of each component in the experimental design. The bottom left corner represents the area of minimal stripping.

3.2 Contrast curve and topography results

Contrast curve generation (Figure 5) using a 248-nm filtered broadband light source indicated that the BARC film does have positive-working, photosensitive behavior. Using the same experimental procedure, it was demonstrated that the BARC film is able to develop out of tight spaces at exposure doses greater than 10 mJ/cm^2 (Figure 6).

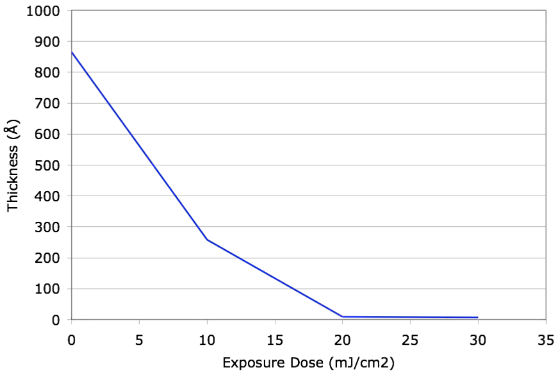

Figure 5. Contrast curve of BARC obtained from using broadband light source with 248-nm bandpass filter.

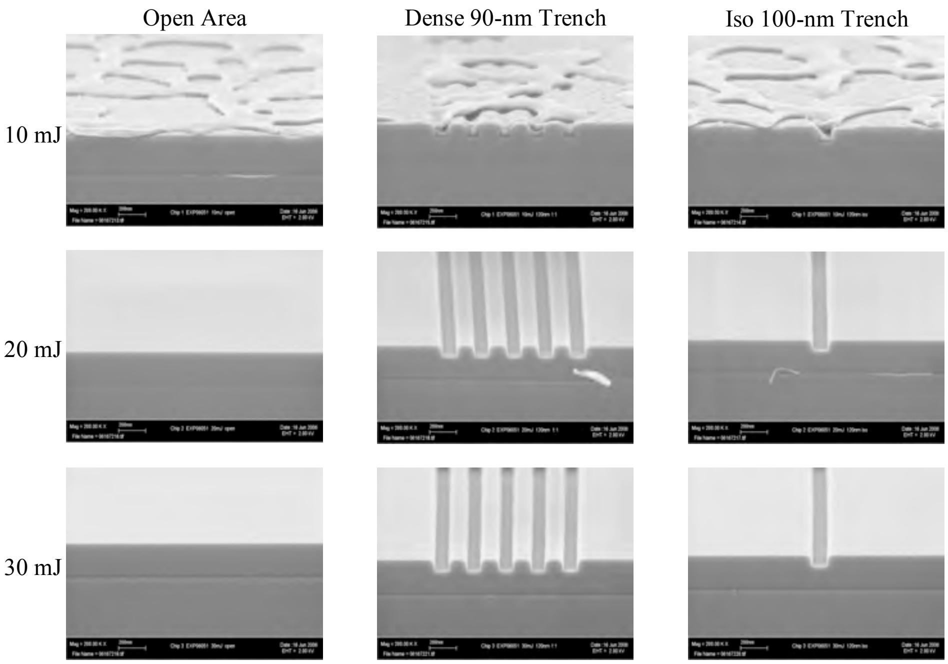

Figure 6. Cross-section images of topography showing BARC behavior after different exposure doses.

3.3 Lithographic evaluation

The reflectivity curve on silicon was generated using PROLITH. Based on prior work on 193-nm photosensitive BARCs,[6] it was determined that performance would be evaluated at the first maximum reflectivity thickness. The reflectivity curve is shown in Figure 7.

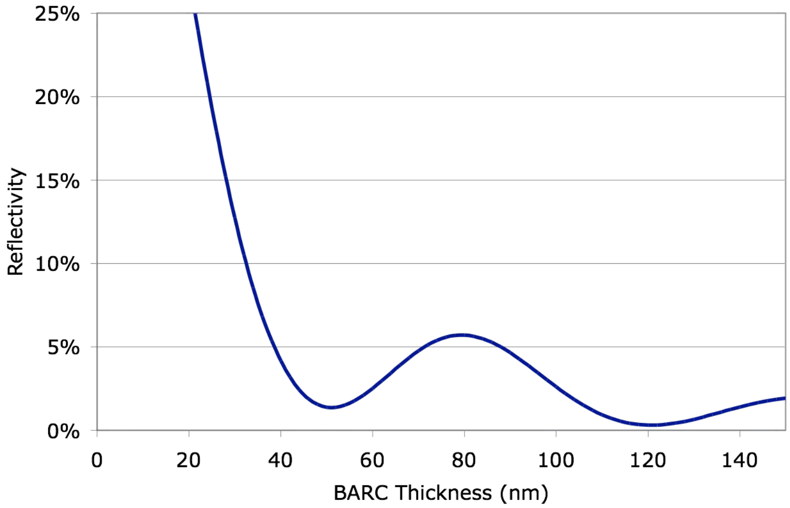

Figure 7. Reflectivity curve on silicon for 248-nm BARC formulation.

While the design solution was able to perform well lithographically at the first maximum reflectivity thickness of 80 nm to give 150-nm (1:1 L/S) resolution (Fig. 8a), the cross-sections showed a significant amount of BARC-resist interaction. It appears that the resist was being poisoned by the BARC, as it never fully clears and leaves a thin layer of resist at the BARC interface (Fig. 8b).

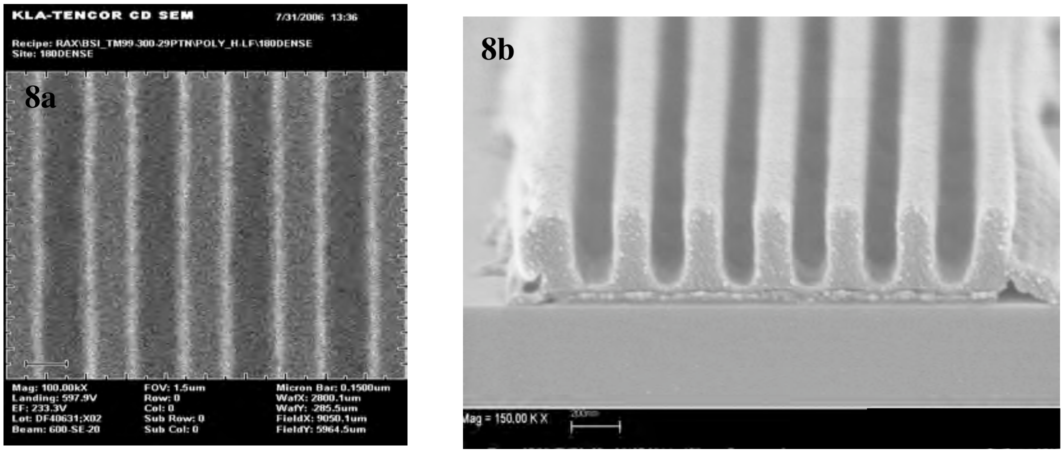

Figure 8. SEM images of 150-nm (1:1 L/S) features obtained from M91Y and 248-nm BARC formulation.

3.4 Effect of polymer

The effect of the polymer on the lithographic performance was also investigated. Two similar polymer binders were prepared, with polymer 1 containing a phenyl unit, and polymer 2 containing an alicyclic unit in place of the phenyl unit. The properties of each polymer are shown in Table 3.

Table 3. Polymer properties comparison.

	Polymer 1	Polymer 2
Molecular Weight	16,100	18,050
n at 248 nm	1.6301	1.586
k at 248 nm	0.0024	0.0012

There were no appreciable differences obtained in the measurement of depth of focus (DOF) for 180-nm CD (1:1 L/S), shown in Figure 9. These findings are not unexpected, as the photoresist and the processing are identical. However, a marked performance increase is obtained in the measurement of exposure latitude between the two polymers (Figure 10). Polymer 1 shows larger exposure latitude than polymer 2. Possible explanations for this observation are that the presence of the phenyl rings in the polymer backbone (polymer 1) induces energy transfer to the PAG in the BARC and resist.[11] It has also been suggested that more polar polymer matrices (in this case, polymer 1) enhance the rate of deprotection in resist systems by stabilizing ionic intermediates and highly polar transition states.[12] Although this is not a resist system, there is evidence of close BARC-resist interaction in the SEM cross-sections (Fig. 8b), and the decrosslinking mechanism can be likened to a photoresist deprotection transition state.

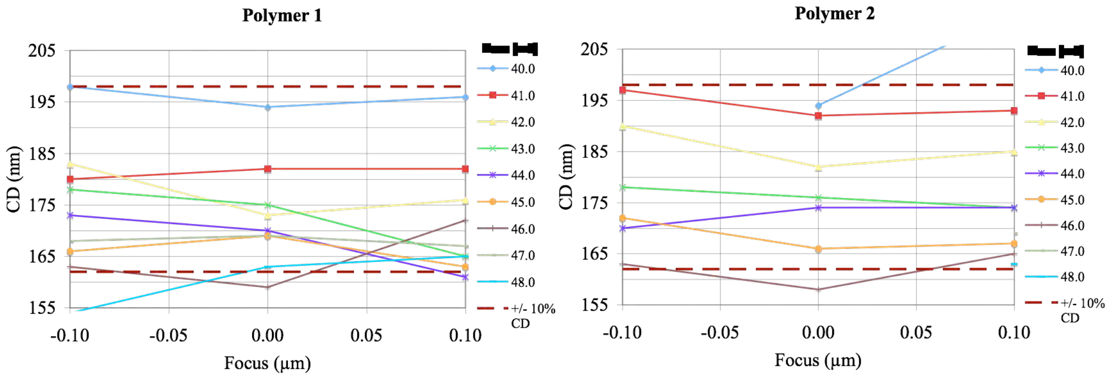

Figure 9. DOF measurements for similar BARC formulations with differing polymer binders.

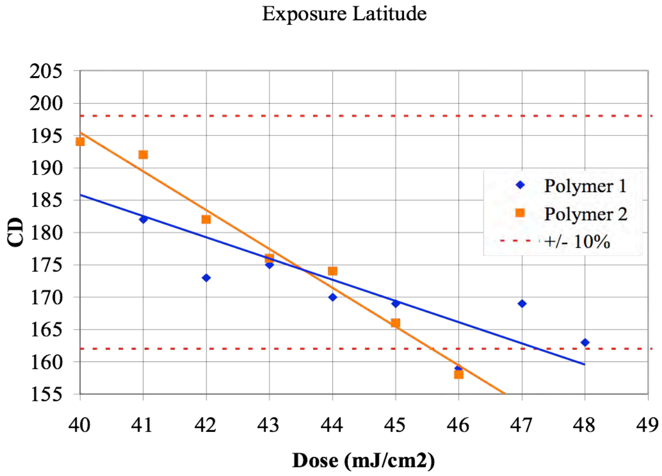

Figure 10. Exposure latitude measurements for similar BARC formulations with differing polymer binders.

4. CONCLUSIONS

The novel approach of combining a transparent polymer binder, oligomeric dye, crosslinker, PAGs, and quencher to develop a photosensitive, developer-soluble BARC was demonstrated. The BARCs are soluble in industry-accepted solvent systems. These BARCs have sufficient *k* values to reduce the substrate reflectivity sufficiently such that small CDs are achieved. The BARC films are able to clear out of small spaces given a sufficient exposure dose. However, much more optimization needs to be done in order to ensure compatibility with photoresists for KrF lithography.

REFERENCES

1. Owe-Yang, D.C.; Ho, B-C.; Miyazaki, S.; Katayama, T.; Susukida, K.; Kang, W. and Y.-C. Chang, "Application of photosensitive BARC and KrF resist on implant layers," *Proc. SPIE* 5376, 452-460 (2004).
2. Katayama, T.; Motobayashi, H.; Kang, W.; Toukhy, M.; Oberlander, J.; Ding, S. and M. Neisser, "Developable bottom antireflective coatings for 248nm and 193m, lithography," *Proc. SPIE* 5377, 968-973 (2004).
3. Guerrero, D.J.; Smith, T.; Kato, M.; Kimura, S. and T. Enomoto, "Two-layer anti-reflection strategies for implant applications," *Proc. SPIE* 6153, 242-249 (2006).
4. Cox, C.; Dippel, D.; Ghelli, C.; Valerio, P.; Simmons, B. and A. Guerrero, "Developer soluble organic BARCs for KrF lithography," *Proc. SPIE* 5039, 878-882 (2003).
5. Shao, X.; Guerrero, A. and Y. Gu, Semicon China SEMI Technology Symposium, 2004.
6. Meador, J.; Beaman, C.; Lowes, J.; Washburn, C.; Mercado, R.; Nagatkina, M. and C. Stroud, "Development of 193-nm wet BARCs for implant applications," *Proc. SPIE* 6153, 854-863 (2006).
7. Guerrero, D. and T. Trudgeon, "A new generation of bottom anti-reflective coatings (BARCs): photodefinable BARCs," *Proc. SPIE* 5039, 129-135 (2003).
8. Guerrero, D. J.; Mercado, R.; Washburn, C. and J. Meador, "Photochemical studies on bottom anti-reflective coatings," *J. of Photopol. Sci. and Tech.*, (19) 3, 343-347 (2006).
9. Washburn, C.; Mercado, R.; Washburn, C. and J. Meador, "Controlling CD and process window limits for implant patterning," *Solid State Technology*, 49(10), 53-56 (2006).
10. Guilmeau, I.; Guerrero, A. F.; Blain, V.; Kremer, S.; Valchellerie, V.; Lenoble, D.; Nogueira, P.; Mougel; S. and J.-D. Chapon, "Evaluation of wet-developable KrF organic BARC to improve CD uniformity for implant application," *Proc. SPIE* 5376, 461-470 (2004).
11. Allen, R. D.; Opitz, J.; Larson, C. E.; Wallow, T. I.; DiPietro, R. A.; Breyta, G.; Sooriyakumaran, R.; Hofer, D. C., "The Influence of Photoacid Structure on the Design and Performance of 193-nm Resists," *J. of Photopol. Sci. and Tech.*, (10) 3, 503-510 (1997).
12. Pohlers, G.; Barclay, G.; Razvi, A.; Stafford, C.; Barbieri, T.; and Cameron, J., "Why do weak acids not work in 193-nm photoresists? Matrix effects on acid catalyzed deprotection," *Proc. SPIE* 5376, 79-93 (2004).